Journal of Physiology (1993), **471**, *pp.* 729–748
With 6 figures
Printed in Great Britain

SYNAPTIC- AND AGONIST-INDUCED CHLORIDE CURRENTS IN NEONATAL RAT SYMPATHETIC PREGANGLIONIC NEURONES *IN VITRO*

BY J. KRUPP AND P. FELTZ

From the Institut de Physiologie (URA 1446 CNRS), Université Louis Pasteur, 21 rue René Descartes, 67084 Strasbourg Cedex, France

(*Received 2 July 1992*)

SUMMARY

1. By using the whole-cell recording configuration of the patch-clamp technique in a spinal cord slice preparation, we have made recordings from visually identified neurones in the lateral horn of the thoracic and lumbar spinal cord of neonatal rats (newborn to 14 days postnatal).

2. Some of the recorded neurones were labelled with the fluorescent dye Lucifer Yellow ($n = 27$). Their morphology was typical for sympathetic preganglionic neurones (SPNs). Based on the size of the cell soma and the electrophysiological properties, unlabelled neurones were also regarded as SPNs.

3. Spontaneous synaptic activity of different patterns could be observed in 73% of the recorded neurones ($n = 106$). It reversed at the chloride equilibrium potential (E_{Cl}) and could be reversibly blocked by strychnine (1–10 μM), but not by bicuculline (10 μM) or SR95531 (5–10 μM).

4. Synaptic activity could be elicited by focal electrical stimulation in the vicinity of the recorded neurone. These evoked synaptic events exhibited features similar to the spontaneous synaptic activity.

5. Application of glycine (100 μM–1 mM) by a fast microperfusion system induced a chloride current in twenty-seven out of thirty cells tested. The currents were reversibly blocked by strychnine (1–10 μM), but were only weakly sensitive to bicuculline (10 μM). Stability of current responses to glycine was increased by inclusion of ATP (4 mM) in the intracellular medium.

6. Application of γ-aminobutyric acid (GABA; 100 μM–1 mM) by the fast microperfusion system induced a chloride current in all twenty neurones tested. These currents were reversibly blocked by bicuculline (10 μM). Strychnine (1–10 μM) blocked this current only weakly. Run-down of GABA-induced currents was prevented to a great extent by inclusion of ATP (4 mM) in the pipette.

7. These results suggest that the inhibitory synaptic activity recorded from SPNs in thin, transverse slices of neonatal rat spinal cord is mediated by glycine receptor-gated Cl^- channels. $GABA_A$ receptor-gated Cl^- channels might be activated by inputs from other spinal segments and/or descending pathways from higher brain regions.

INTRODUCTION

In mammals sympathetic preganglionic neurones (SPNs) are mainly located in the intermediolateral cell column (IML) of thoracic and lumbar spinal cord, where they receive inputs from many regions of the CNS (Laskey & Polosa, 1988), e.g. the raphé nuclei (Henry & Calaresu, 1974; Bacon, Zagon & Smith, 1990), the catecholaminergic A5 cell group (Loewy, McKellar & Saper, 1979) or the parvocellular paraventricular hypothalamic nucleus (Saper, Loewy, Swanson & Cowan, 1976; Swanson, 1977). SPNs integrate the information of these sources and lead it – directly or via sympathetic postganglionic neurones – to its targets in the body periphery.

To fulfil this function, the excitability of SPNs seems to be regulated by an interplay of various neurotransmitters (for review see McCall, 1988). In this context, we were interested in the inhibitory inputs that act on SPNs.

It is well known that the amino acids glycine and γ-aminobutyric acid (GABA) both inhibit the electrical activity of SPNs (Yoshimura & Nishi, 1982; Backman & Henry, 1983). GABA-immunoreactive axons have been shown to synapse directly onto SPNs (Bogan, Mennone & Cabot, 1986; Bacon & Smith, 1988) and GABA as well as glycine or glycine receptor immunoreactivity can be found in the IML (Chiba & Semba, 1991; Cabot, Alessi & Bushnell, 1992). Indeed, glycine seems to be responsible for inhibitory postsynaptic potentials (IPSPs) recorded in SPNs of a spinal cord slice preparation with conventional intracellular electrodes (Mo & Dun, 1987). Interneurones that can be activated by *N*-methyl-D-aspartate (NMDA) are proposed to release glycine onto SPNs (Dun & Mo, 1989).

In the present study, we have used the patch-clamp technique (Hamill, Marty, Neher, Sakmann & Sigworth, 1981) in sliced preparations (Edwards, Konnerth, Sakmann & Takahashi, 1989) to investigate the ionic nature of the inhibitory synaptic events in SPNs and the action of glycine and GABA on these neurones.

METHODS

Preparation of slices

The procedures to obtain thin spinal cord slices (200–300 μm) in general followed the descriptions given by Takahashi (1978, 1990) and are briefly described below. Neonatal Wistar rats (newborn to 14 days postnatal) were anaesthetized with ether prior to performing a laminectomy. The spinal cord was quickly removed and submerged in oxygenated (95% O_2/5% CO_2), ice-cooled (4 °C) artificial cerebrospinal fluid (ACSF) of the composition given below (see *Solutions*). Using fine scissors and forceps the pia mater was gently removed under binocular vision. The spinal cord was subdivided into several 0·5 cm blocks using a sharp razor blade. One block was embedded in fresh, cool (< 38 °C) agar (2·5%) that was then rapidly solidified by application of ice-cooled ACSF. The piece of solidified agar containing the spinal cord part was glued onto the bottom of a Petri dish with cyanoacrylate glue. The dish was fixed to a vibratome (Oxford Vibratome Series G) and filled with ice-cooled ACSF. The first slice was discarded. Slices sucked up with a glass pasteur pipette were immediately transferred to a storing chamber filled with room-temperature, oxygenated ACSF. After recovery for at least 1 h, one slice was transferred to a glass-bottomed recording chamber. The slice was held by a nylon mesh glued to a U-shaped silver wire (Edwards *et al.* 1989). The chamber (volume: 0·8 ml) was continuously perfused with warm (33±3 °C), oxygenated ACSF at a rate of about 4 ml min^{-1}.

Solutions

The ACSF used throughout the experiments had the following composition (mM): NaCl, 113; KCl, 3; NaH_2PO_4, 1; $NaHCO_3$, 25; glucose, 11; $CaCl_2$, 2; $MgCl_2$, 1; pH 7·4 when bubbled with 95%

O_2/5% CO_2. When using Ca^{2+}-free solution, $CaCl_2$ was omitted from the solution and $MgCl_2$ was augmented to 5 mM. In general, two different intracellular solutions have been used in the experiments. In the first part of this paper dealing with the characteristics of the described synaptic currents, a potassium-based solution of the following composition was used (mM): KCl, 140; NaCl, 9; $MgCl_2$, 1; Hepes, 10; EGTA, 0·2; pH 7·3 (KOH). To test the ionic nature of the observed currents, KCl was substituted by: (1) (mM) potassium D-gluconate, 29; KCl, 111; (2) (mM) potassium D-gluconate, 103; KCl, 37; or (3) (mM) potassium D-gluconate, 130; KCl, 10. ATP-containing intracellular solutions used in the second part of this paper were prepared with (mM): CsCl, 120; TEA–Cl, 20; $MgCl_2$, 2; Hepes, 10; EGTA, 10; $CaCl_2$, 1; Na_2ATP, 4; pH 7·3 (CsOH). For later examination of cell morphology and identification as SPNs some electrode solutions contained in addition the fluorescent dye Lucifer Yellow (1–2 mg ml^{-1}).

Application of drugs

All drugs were purchased from Sigma (France), except bicuculline methiodide (Pierce Chemical Co., IL, USA), 6-cyano-7-nitroquinoxaline-2,3-dione (CNQX) (Tocris Neuramin, UK) and SR 95531 (Sanofi Recherche, France).

Agents could be tested in two different ways. One was to apply the drug dissolved in ACSF by conventional superfusion driven by gravity. This application method needed a few minutes to reach an equilibrium state. It was used when applying receptor antagonists like strychnine or bicuculline. The second method used a fast microperfusion system consisting of a manipulator-mounted barrel of small plastic pipettes with inner tip diameters of 350 μm (Polylabo, France). They were connected via silicone tubing to syringes containing the drug dissolved in ACSF some 10 cm higher than the recording chamber. The outflow from the tip could be interrupted by a valve. To avoid seal disruption, the tips of the micropipettes were placed 500–1000 μm away from the cell. $NaHCO_3$ was replaced by Hepes (5 mM; pH 7·4 with NaOH) as the buffer in drug solutions to prevent formation of bubbles in the microperfusion system which would impede drug solution flow. Moreover, to indicate if the drug had reached the recorded cell, Phenol Red (50 μM) was added to this ACSF. Control experiments showed that no electrical responses were elicited after application of ACSF which had been changed in this way.

The speed and accuracy of the solution exchange was tested in the following way. The microperfusion system was filled with a 50:50 mixture of ACSF and distilled water. After adjustment of the microperfusion system, a patch electrode was lowered on top of and 30 μm into the slice, which is approximately the depth at which seals were made in the experiments. The pressure in the pipette was released. A square-wave signal (100 Hz) was applied to the electrode and the change in electrical conductivity determined before and after the opening of the valve of the microperfusion system. When we normalized to the mean conductivity before opening the valve, we observed a steady-state decrease of the normalized conductivity to $0·71 \pm 0·02$ ($n = 33$) and $0·92 \pm 0·06$ ($n = 99$) at the surface and 30 μm into the slice, respectively. There were no significant differences in the steady-state levels between the three pipettes. As the theoretical maximal change of conductivity would be a decrease of normalized conductivity to 0·5, the values indicate that in the experiment the concentration of the respective drug reaching the cell is about 0·58 and 0·17 times the concentration of the drug in the pipette solution for the surface and 30 μm into the slice, respectively.

Stimulation

To record electrically evoked responses, two nearby cells (100–200 μm distance) were selected. The stimulation electrode, being a regular patch pipette filled with ACSF and having a resistance of 1–5 MΩ, was lowered onto the surface of one of the selected cells. After the whole-cell recording configuration had been established with the patch electrode recording from the second cell, a voltage pulse (200 μs, 2 Hz) was delivered between the stimulation electrode and a bath electrode. The voltage was increased (4–20 V) until a response was seen in the recorded cell.

Recording conditions and analysis

Experiments were performed using an upright microscope (Zeiss Axioskop FS) with water immersion optics (×40 objective, Zeiss, Germany). Patch pipettes for whole-cell recording (Hamill *et al.* 1981) were pulled on a L/M-3P-A puller (List Electronics, Darmstadt, Germany) from Pyrex glass (o.d., 1·55 mm; wall thickness, 350 μm). They had resistances of 2–5 MΩ when filled with intracellular solution. Recordings made using an EPC-5 amplifier (List Electronics) were filtered at

3 kHz (filter on EPC-5) and stored on magnetic tape (Racal recorder, UK) with a bandwidth of 1·25–10 kHz. Off-line analysis was performed by using the program pClamp 5 (Axon Instruments, USA) and an analysis program for spontaneous synaptic events written by P. Vincent (Paris, France). Traces were plotted on paper using a chart recorder (Gould 2200S) or a Hewlett–Packard plotter (HP 7470A) in combination with pClamp 5.

Examination of cell morphology

When cells had been labelled with Lucifer Yellow slices were transferred to a fixation medium (4% formaldehyde with 0·1 mM phosphate buffer) after the experiments and stored overnight in the refrigerator. The following day slices were cleared for 10–15 min in dimethyl sulphoxide (Grace & Llinás, 1985), placed on microslides and covered with coverslips. After mounting, the slices were viewed under blue light epifluorescence, using a Zeiss filter combination (band-pass filter for excitation, 450–490 nm; band-pass filter for emission, 515–565 nm) for Lucifer Yellow fluorescence and photographed.

Conventions

Inward currents are downward in all figures. All results are expressed as means ± standard deviation. In Figs 2*B*, 2*D*, 5*A* and 6*A* mean peak current amplitudes and means of standard error are indicated by symbols and bars, respectively.

RESULTS

Morphology of recorded cells

All cells injected with Lucifer Yellow ($n = 27$) were located in the lateral horn. They had an oval or fusiform shape with their long axis mostly orientated mediolaterally. The diameter of the cells was $26{\cdot}1 \pm 3{\cdot}9 \times 17{\cdot}2 \pm 1{\cdot}4$ μm. The cell nucleus was big and was about half to two-thirds of the size of the somata. The dendrites of the cells showed a typical arrangement with one or more long dendrites extending towards the central canal. Generally, shorter dendrites could also be seen extending towards the lateral funiculus. In accordance with previous studies (Cabot & Bogan, 1987; Shen & Dun, 1990) dendrites had a beaded appearance, due to the occurrence of varicosities. This may, however, at least partially also be due to an overexposure of the slices to fluorescent light. The cell axon was in general thinner and less beaded. It arose either at the ventrolateral edge of the cell or close to a proximal dendrite, and took its course along the border of the white and grey matter towards the ventral root. Figure 1 shows an example of a neurone exhibiting this arrangement.

The described morphology was shown to be typical for SPNs in the lateral horn (Forehand, 1990; Shen & Dun, 1990) and has already been used as a criterion for positive identification of these neurones by other authors (Pickering, Spanswick & Logan, 1991). In addition, we have been able to label SPNs retrogradely (Y. Larmet, J. Krupp & P. Feltz, unpublished observations) after injection of 1,1′-dioctadecyl-3,3,3′,3′-tetramethylindocarbo-cyanine perchlorate (DiI) into the adrenal medulla. The location, size and morphology of these identified SPNs were similar to those of the cells injected with Lucifer Yellow in this study.

Neurones recorded with electrodes containing no Lucifer Yellow were chosen under visual control. They were located in the lateral horn, had cell soma diameters of 20–28 μm and a mediolateral orientation of their long axes. No difference in the described electrophysiological properties could be detected between labelled and unlabelled neurones.

Inhibitory synaptic events

Recordings were included in this study only when either the neurones had resting membrane potentials more negative than −40 mV when recorded with a KCl intracellular solution, or if the recording was stable for at least 20 min when

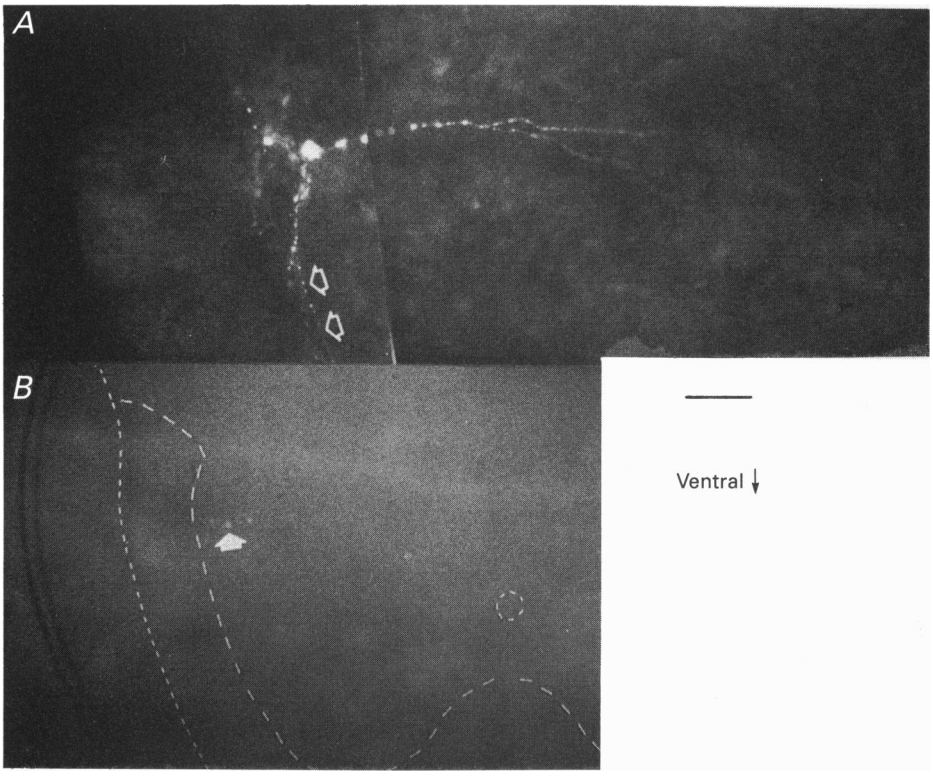

Fig. 1. Location and morphological appearance of SPNs. *A*, photo-montage of a neurone stained with Lucifer Yellow (1·3 mg ml^{-1}) in a transverse rat spinal cord slice. One dendrite can be seen to extend medially towards the central canal. This dendrite divides into two branches in its final course. Smaller dendrites orientate towards the lateral funiculus. One extension, probably the axon (light arrowheads), leaves the soma close to a major dendritic tree and travels along the border of the white and grey matter. At the ventral edge of the horn it turns towards the white matter, but is cut shortly afterwards (not shown). Calibration bar is 100 μm. The beaded appearance of the dendrites can be explained by the occurrence of varicosities, but may also result from overexposure of the slice to fluorescent light. *B*, location of the same neurone as in *A* (arrow) in the lateral horn. The central canal and the borders of slice, as well as the white and grey matter, are indicated by the dashed line. Calibration bar is 230 μm.

using a CsCl intracellular solution. Using these criteria, whole-cell recordings were obtained from a total of 106 neurones. When using a KCl intracellular solution, neurones had a mean resting membrane potential of $-60{\cdot}2 \pm 14{\cdot}3$ mV ($n = 61$). Their mean input resistance was 981 ± 160 MΩ ($n = 9$) and their mean capacitance $32{\cdot}3 \pm 12{\cdot}2$ pF ($n = 11$). The recordings from seventy-eight neurones (73%) showed

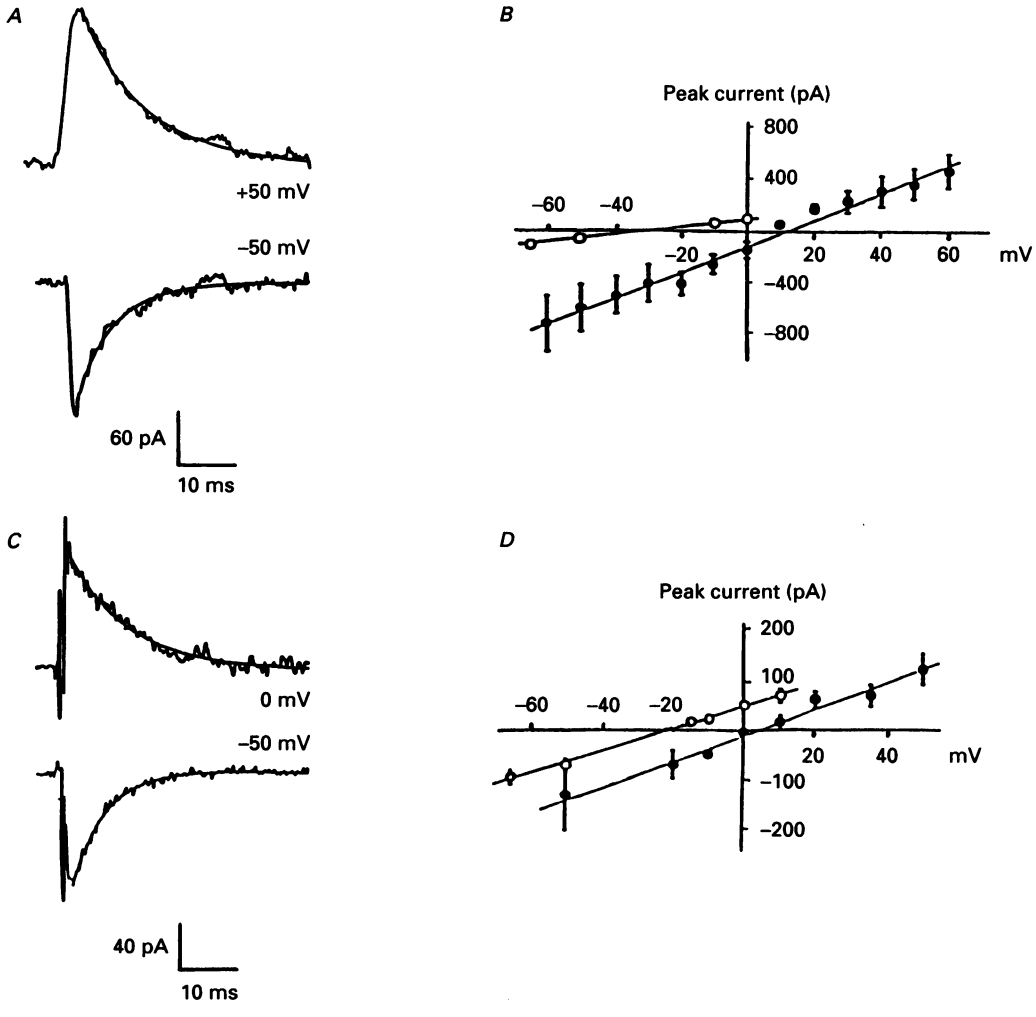

Fig. 2. Comparison of spontaneous and evoked synaptic currents. *A*, spontaneous synaptic currents of a neurone held at the potentials indicated on the current traces. The decaying phase of the spontaneous currents can be fitted with a single exponential having a time constant (τ) of 6·35 ms and a peak current amplitude (A_0) of −152·5 pA at V_h = −50 mV. At a V_h of +50 mV the values are τ = 10·6 ms and A_0 = 198·4 pA (E_{Cl} = 0 mV). *B*, *I–V* relationship of spontaneous synaptic currents. The relationship is linear and the currents reverse polarity at 11·8 mV (E_{Cl} = 6 mV; ●) and −30·9 mV (E_{Cl} = −25 mV; ○). *C*, evoked synaptic currents of a neurone held at the potentials indicated on the current traces. The decaying phase of the currents can be fitted with a single exponential with τ = 5·88 ms and A_0 = −105·8 pA at V_h = −50 mV or τ = 10·11 ms and A_0 = 104·5 pA at V_h = 0 mV (E_{Cl} = −25 mV). Stimulus was 8 V for 200 μs (2 Hz). *D*, *I–V* relationship of evoked synaptic currents. The relationship is linear. Currents reverse polarity at 4·7 mV in equimolar Cl^- solution (●) and −21 mV (E_{Cl} = −25 mV; (○). Recording bandwidth was 2·5 kHz.

monophasic events – currents as well as potentials – that occurred spontaneously (Fig. 2*A*). In the voltage-clamp mode and at the standard holding potential (V_h) of −50 mV the currents were inward under symmetrical Cl^- conditions. They had

amplitudes ranging from less than 20 pA up to 2 nA. The monophasic currents were reduced, both in amplitude and frequency, in Ca^{2+}-free ACSF ($n = 3$) or after application of TTX (1 μM) to the bath ($n = 4$). Only miniature monophasic events were left under these conditions. The spontaneous monophasic events were thus considered to be synaptically mediated.

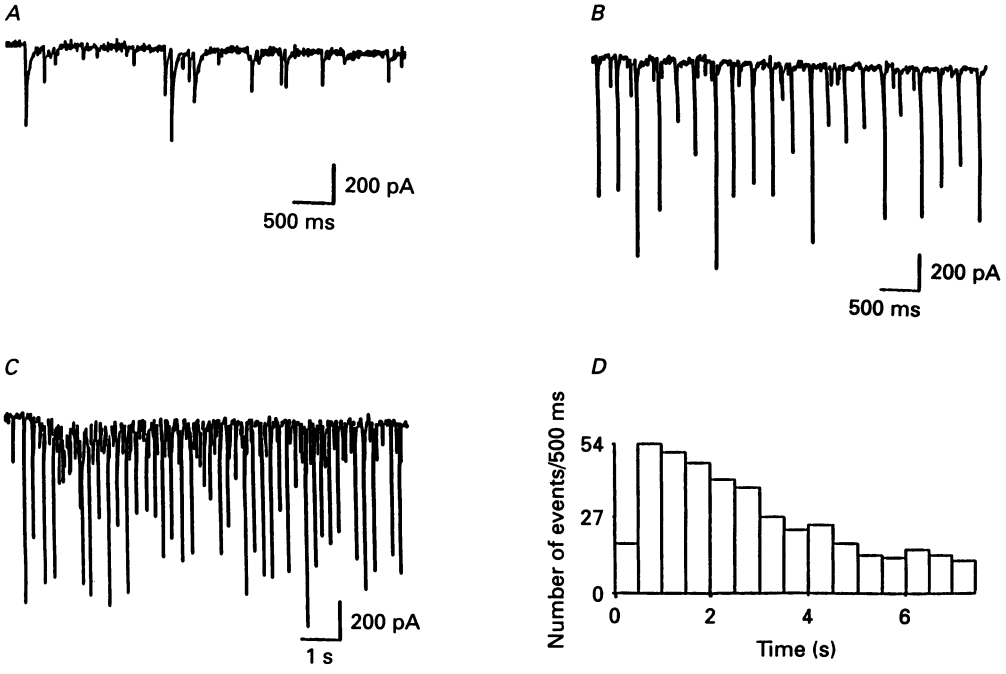

Fig. 3. Different patterns of spontaneous synaptic activity. *A*, synaptic currents in one neurone occurring in an irregular manner with a mean frequency of 4 Hz. *B*, regular synaptic currents recorded in another neurone that also displayed irregular events. The regular synaptic events occur at a frequency of 4 Hz; the overall mean frequency is 9 Hz. *C*, synaptic currents exhibiting a transient, high-frequency pattern in the same cell as in *B*. *D*, histogram showing the frequency decrease with time of the spontaneous synaptic pattern illustrated in *C*. In each case $V_h = -50$ mV. Note the different time scale in *C*.

Synaptic activity could be mimicked by electrical stimulation (Fig. 2*C*). The latency of these evoked synaptic currents following stimulation was short (< 1 ms) and the response usually began to rise before the stimulus artifact was terminated (Fig. 2*C*). Therefore the rise time of evoked synaptic currents could not be measured directly. The extrapolated base-to-peak rise time was $1{\cdot}4 \pm 0{\cdot}6$ ms ($n = 6$). This was the same as the directly measured base-to-peak rise time of spontaneous synaptic currents, which was $1{\cdot}4 \pm 0{\cdot}5$ ms ($n = 31$). The decaying phase of the spontaneous as well as the evoked synaptic currents could in most cases be fitted by one exponential. Spontaneous synaptic currents had a time constant of $\tau_{spont} = 8{\cdot}5 \pm 5{\cdot}3$ ms (thirty events from three cells at $V_h = -50$ mV; range 3–18 ms), and the evoked synaptic currents had a time constant of $\tau_{evoked} = 7{\cdot}6 \pm 3{\cdot}0$ ms (ten averaged traces, ten events

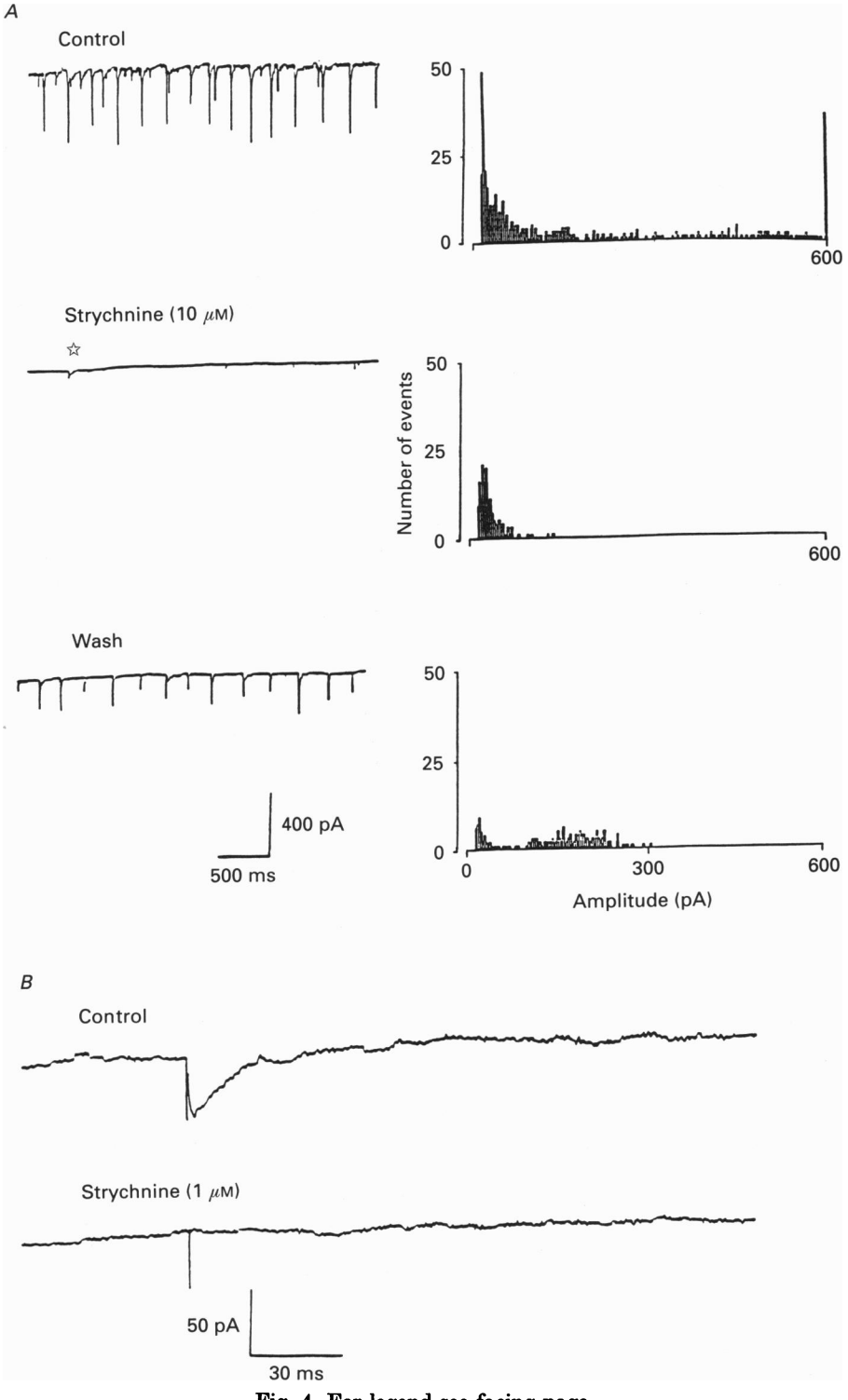

Fig. 4. For legend see facing page.

each, from four cells at $V_h = -50$ mV). τ was weakly sensitive to voltage and increased with depolarization. The decaying phase of the observed synaptic currents could sometimes also be fitted by two exponentials. As this may be due to the interference with unblocked synaptic currents other than the one described here, these currents were not included in this study.

The current–voltage (*I–V*) relationships of evoked and spontaneous synaptic currents were comparable. As illustrated in Fig. 2*B* and *D* the *I–V* relationship was linear. The reversal potential could be shifted along the voltage axis as expected from the Nernst equation for a current carried by chloride ions. When recording spontaneous synaptic currents with an intracellular solution that gave an equilibrium potential for chloride (E_{Cl}) of 6 mV, currents reversed at 11·8 mV (● in Fig. 2*B*) for the example given, with a mean of $10{\cdot}4 \pm 1{\cdot}5$ mV ($n = 3$) in the cells thus examined. Upon shifting the E_{Cl} to -25 mV, the measured reversal potential was $-30{\cdot}9$ mV (○ in Fig. 2*B*). The evoked synaptic currents (Fig. 2*D*) reversed at 4·7 mV in equimolar chloride solution (●) for the example given and had a mean reversal potential of $4{\cdot}0 \pm 1{\cdot}4$ mV ($n = 4$). When E_{Cl} was fixed to -25 mV (○) the reversal potential of the evoked synaptic currents was -21 mV.

In most recordings the spontaneous synaptic activity was irregular (Fig. 3*A*), ranging from less than 0·1 to 20 Hz. The frequency of the irregular synaptic events often decreased during the recording, sometimes disappearing completely after 30 min. The synaptic activity of four neurones displayed a very sustained and rhythmic pattern (Fig. 3*B*). These currents were larger than most of the synaptic currents observed in cells with irregular synaptic activity. The frequency of the regular synaptic activity ranged from 1 to 10 Hz, occasionally reaching 20 Hz. The frequency normally did not decrease throughout the recording period (> 2 h). Both

---

Fig. 4. Effects of strychnine on spontaneous and evoked synaptic activity. *A*, chart traces (left) illustrating the effect of strychnine (10 μM) on spontaneous synaptic activity and their respective amplitude histograms (right). Prior to application of strychnine (top trace), the mean frequency of events is 15 Hz and the mean peak amplitude -195 pA. Most of the events are blocked during the application of strychnine (middle trace). The mean frequency is now 5 Hz and the mean peak amplitude -37 pA. The respective amplitude histogram concentrates onto small and fast decaying ($\tau = 1{\cdot}4$ ms) synaptic events with amplitudes of about -50 pA. Due to their fast time course they appear as a single inward line on the chart trace. Comparable synaptic currents in other SPNs could be blocked by CNQX (5 μM). The trace also shows a single synaptic event that has a time course comparable to the synaptic events of the control (☆). After 30 min of wash-out of strychnine (lower trace), the regular, bigger synaptic currents blocked by strychnine have reappeared. Although their amplitudes indicate that they have not yet completely recovered from block, their frequency is nearly the same as under control conditions. Note also that the baseline noise is still low. The amplitude histogram reveals two distinct distributions. The mean frequency of the events is 6 Hz; their mean peak amplitude is -140 pA. V_h was -50 mV in each case. Same calibration for all traces. For the sake of comparison the shell is equal for all three histograms. Bin width for all panels is 3 pA. Amplitude histograms were constructed by analysing a representative 30 s trace of the respective record. The 600 pA bin for control conditions comprises all events equal to or bigger than 600 pA. Due to the limited dynamic range of the pen-recorder the sizes of synaptic currents are truncated. *B*, evoked synaptic currents before (top) and during (bottom) application of strychnine (1 μM). Each trace is the average of six consecutive traces. $V_h = -50$ mV.

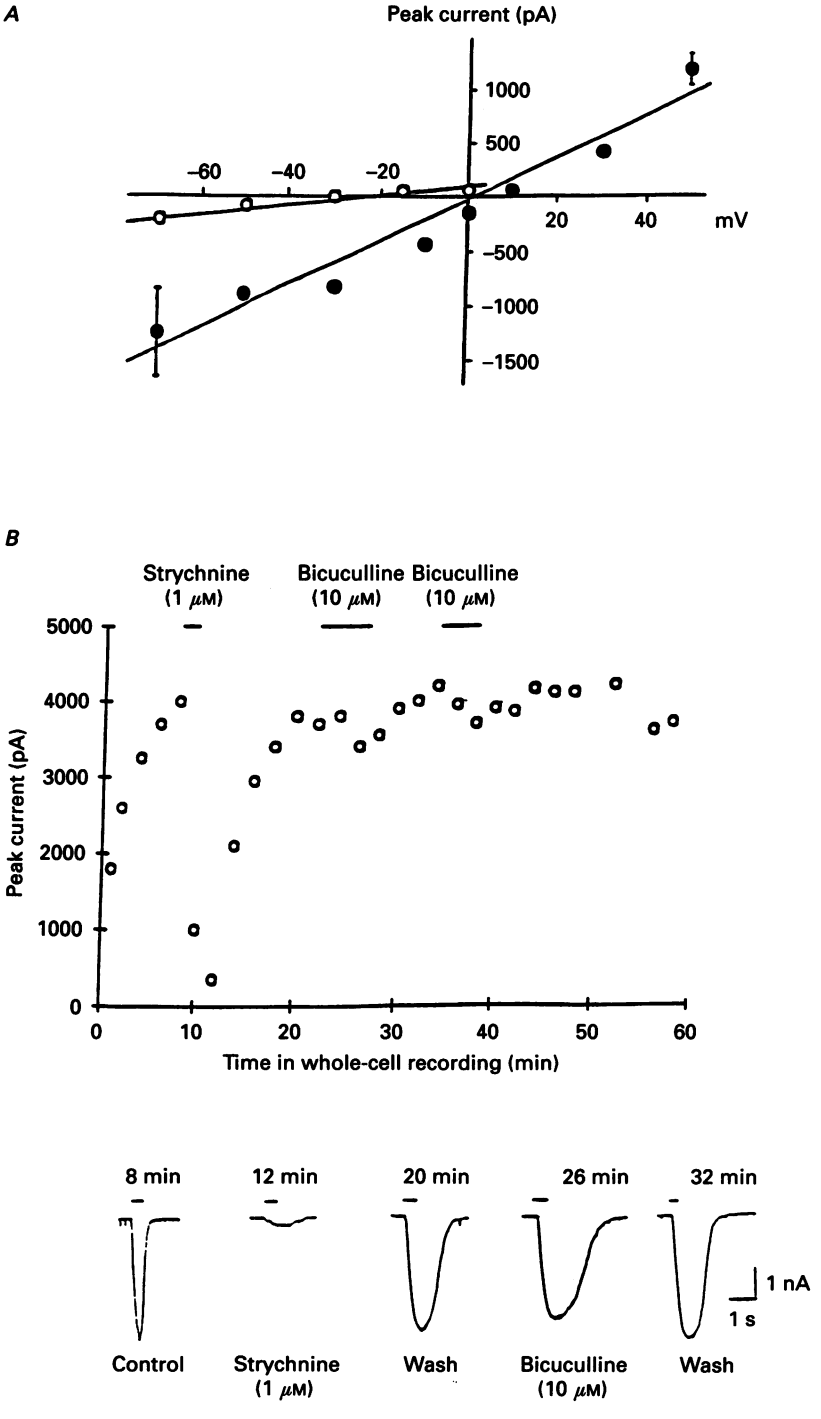

Fig. 5. For legend see facing page.

patterns have previously been described for SPNs by Dun & Mo (1989) using conventional intracellular recording. In addition, a third type of synaptic activity could be observed in some neurones (Fig. 3*C*). It consisted of a transient (1–7 s), high-frequency (20–100 Hz) discharge of synaptic events and could be found to be associated both with the irregular as well as the regular pattern. The frequency of synaptic events often decreased continuously throughout such a burst (Fig. 3*D*). This type of synaptic activity was usually only observed during the first 30 min of recording.

Most of the spontaneous synaptic activity was blocked by superfusing the preparation with the glycine receptor antagonist strychnine (1–10 μM) in all five cells tested. Figure 4*A* shows the blocking effect of strychnine in one of the cells exhibiting the regular synaptic activity. However, some small synaptic currents remained (middle trace). Compared to control levels, their frequency was reduced and their peak current amplitudes were never bigger than 100 pA. These small synaptic currents decayed faster than the large synaptic currents blocked by strychnine (τ = 1·4 ± 2·6 ms; n = 20). At a V_h of −50 mV these strychnine-insensitive synaptic events could be blocked by the non-NMDA receptor antagonist CNQX (5 μM; J. Krupp & P. Feltz, unpublished observations).

Even after 30 min of wash-out (lower trace) only a partial recovery occurred. The respective amplitude histogram revealed two distinct distributions. One comprised bigger synaptic currents with an average of about −200 pA. Although the overall frequency of the events was still as low as under strychnine, these bigger currents had nearly the same frequency (of about 4 Hz) as under control conditions. In contrast, the number of small synaptic currents had further decreased compared to the levels under strychnine. This might be explained by masking of the small currents by the large ones.

We did not observe any change in spontaneous synaptic activity after adding $GABA_A$ receptor antagonists such as bicuculline (10 μM; n = 4) or the pyridazinyl GABA compound SR95531 (5–10 μM; n = 3), which has been shown to be a competitive $GABA_A$ receptor antagonist (Hamann, Desarmenien, Desaulles, Bader & Feltz, 1988), to the superfusing bath medium. Also, SR95531 had no effect on the synaptic activity after addition of 4-aminopyridine (4-AP; 100 μM) to the bath (n = 2), which induced an increase in frequency of synaptic events.

As shown in Fig. 4*B*, strychnine (1 μM) also affected the evoked synaptic activity in all neurones tested (n = 4). In general, a complete block of the evoked synaptic currents was observed, both at negative and at positive holding potentials. In one cell, however, a small, slow component was insensitive to strychnine at positive holding potentials, but was abolished by addition of the NMDA receptor antagonist

Fig. 5. Characterization of responses to glycine applied by fast microperfusion. *A*, *I–V* relationship of transmitter-induced peak currents in different cells with solutions that gave an E_{Cl} of 0 mV (●) and −25 mV (○). *B*, pharmacological properties of currents induced by glycine. Graph shows the peak amplitude of glycine-induced currents in relation to time in whole-cell recording. Glycine (100 μM) was applied to the cell by fast microperfusion every 2 min. Open circles represent peak currents of a neurone recorded with intracellular solution containing ATP. The bath application of antagonists is indicated by the bars at the top of the graph. Five traces showing responses before, during and after application of strychnine (1 μM) or bicuculline (10 μM) are illustrated below the graph. V_h = −50 mV.

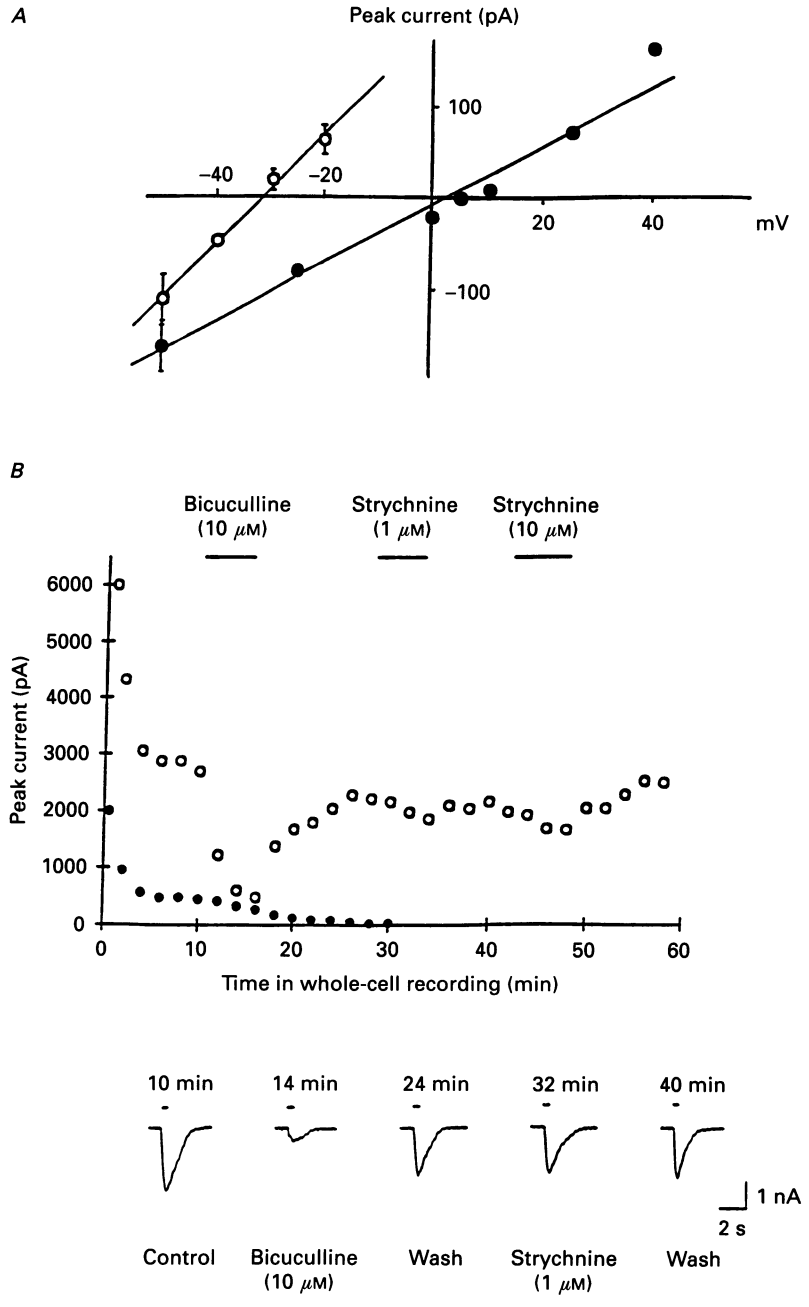

Fig. 6. Characterization of responses to GABA applied by fast microperfusion. *A*, *I–V* relationship of transmitter-induced peak currents in different cells with solutions that gave an E_{Cl} of 0 mV (●) and −25 mV (○). *B*, pharmacological properties and run-down of currents induced by GABA. Graph shows the peak amplitude of GABA-induced currents of two cells in relation to time in whole-cell recording. GABA (100 μM) was applied to the cell by fast microperfusion every 2 min. Points are data obtained from a neurone recorded with ATP-free intracellular solution. Open circles represent peak currents of a neurone recorded with an intracellular solution containing ATP. The bath application of antagonists in the latter recording is indicated by bars at the top of the

DL-2-amino-5-phosphonovaleric acid (40 μM). Bicuculline (10 μM) had no effect on the evoked synaptic currents in the two cells tested.

The previous data indicate that SPNs in a thin, transverse spinal cord slice preparation receive a synaptic input mediated by glycine receptor-gated Cl^- currents. On the other hand, not only glycine, but also GABA have already been shown to inhibit SPN activity (Yoshimura & Nishi, 1982; Backman & Henry, 1983). Indeed, the presence of receptors of the glycine and the $GABA_A$ type has already been shown in dissociated chick embryonic SPNs in culture (Clendening & Hume, 1990). To test the hypothesis that the absence of a spontaneous GABAergic input in the transverse spinal cord slice preparation might be due to the cutting of GABAergic afferents during the slicing procedure, we assayed the activity of exogenously applied glycine and GABA on SPNs.

Effects of glycine

Under whole-cell voltage clamp only three out of thirty neurones were unresponsive to glycine applied by the fast microperfusion system. Nor did these neurones exhibit spontaneous synaptic activity. In the twenty-seven responsive neurones (90%), glycine-induced peak currents were recorded at holding potentials between -70 and $+50$ mV. Figure 5*A* shows the *I–V* relationship for two different neurones recorded with intracellular solutions that gave a theoretical E_{Cl} of 0 mV (●) or -25 mV (○). The measured peak currents in these two neurones reversed at 1 and -19 mV, respectively. In three SPNs recorded under symmetrical chloride conditions, the mean value of the reversal potential was $3{\cdot}0 \pm 2{\cdot}1$ mV ($n = 3$). These results suggest that the currents are mainly carried by chloride ions. Small deviations of the measured reversal potential of glycine-induced peak currents from the theoretical reversal potential for chloride may be explained by a permeability of the glycine receptor-gated channel to ions other than chloride (Bormann, Hamill & Sakmann, 1987). Note especially that during the exogenous application of glycine dissolved in the Hepes-modified ACSF, the concentration of HCO_3^- ions is likely to change. With respect to the chloride dependence and the strychnine sensitivity of this current, our results are in line with the properties of the glycine receptor–Cl^- channel complex reported by other authors for spinal neurones (Clendening & Hume, 1990; Takahashi & Momiyama, 1991; Takahashi, 1992).

Glycine-induced currents often decreased in amplitude with time of whole-cell recording when using an ATP-free intracellular solution. Occasionally, a complete run-down of glycine-induced currents could even be observed when recording with ATP-free intracellular solution. This run-down, as well as the unstable responses, could be largely prevented when using an ATP-containing intracellular solution. Responses to glycine were reversibly blocked by superfusion of strychnine (1–10 μM), whereas bicuculline (10 μM) had only a weak blocking effect on glycine-induced currents (Fig. 5*B*).

---

graph. The fast decline of GABA-induced peak current amplitude in the early phase of the two cases shown is not representative, as it was not consistently observed in all neurones. Five traces showing responses before, during and after application of bicuculline (10 μM) or strychnine (1 μM) are illustrated below the graph. $V_h = -50$ mV.

Effects of GABA

GABA applied to SPNs recorded with an ATP-containing pipette solution under whole-cell patch clamp induced a transient current in all neurones ($n = 20$) tested. The relationship between holding potential and GABA-induced peak currents was tested by changing the holding potential from -50 to $+40$ mV. The I–V relationship for a neurone recorded under symmetrical Cl^- conditions is shown in Fig. 6*A* (●). The reversal potential of GABA-induced peak currents was $-1{\cdot}0 \pm 8{\cdot}6$ mV ($n = 3$). The reversal potential varied with changes in the concentration of chloride in the electrode solution. Therefore, when shifting the theoretical E_{Cl} to -25 mV by decreasing the internal chloride concentration from 122 to 48 mM in one cell, the measured peak currents reversed at $-31{\cdot}5$ mV (○). As for the glycine-induced currents, the small discrepancy between measured GABA-induced peak current reversal potential and theoretical reversal potential for chloride may be due to a permeability of the channel for anions other than chloride (Bormann *et al.* 1987).

When recordings were made with ATP-free intracellular solution, GABA-induced currents showed a complete run-down – mostly within 30 min – that could be slowed remarkably by ATP (Fig. 6*B*). The currents induced by application of GABA could be blocked reversibly by adding bicuculline (10 μM) to the superfusing ACSF (Fig. 6*B*). In addition, strychnine (1–10 μM) also reduced GABA-induced currents, but to a much lesser extent than 10 μM bicuculline (Fig. 6*B*). These results suggest that $GABA_A$ receptors mediated the currents induced by application of GABA (Olsen, 1982; Clendening & Hume, 1990; Schneggenburger, López-Barneo & Konnerth, 1992).

DISCUSSION

Our results demonstrate the involvement of a glycinergic synaptic regulation of SPN activity. Furthermore, they show the presence of functional glycine and $GABA_A$ receptor–Cl^- channel complexes on the membranes of neonatal rat SPNs *in vitro*. Our results support the idea of a differential inhibitory control of SPN activity.

Glycinergic synaptic currents

Sustained spontaneous synaptic activity was observed over recording periods of more than 2 h. Therefore, this regulation probably takes place at an intraspinal level and represents the presynaptic activity of glycinergic interneurones located within the slice. Our results are in line with previous morphological (Cabot *et al.* 1992) as well as electrophysiological findings (Mo & Dun, 1987; Dun & Mo, 1989). Furthermore, they directly demonstrate that chloride is the major current-carrying ion of this intraspinal regulation. Small deviations of the reversal potential of spontaneous and evoked synaptic currents from the theoretical reversal potential for chloride may be explained by the permeability of the glycine receptor-gated chloride channel to other ions (Bormann *et al.* 1987). In fact, as the present study in a slice preparation was performed in oxygenated $NaHCO_3$-containing ACSF, the conditions of recording in a defined chloride gradient could only be approximated.

Although the recorded spontaneous synaptic currents were sometimes quite small and infrequent, the percentage of neurones that exhibited these currents is strikingly high compared to 'rarely observed' IPSPs *in vivo* (Dembowsky, Czachurski & Seller,

1985) and 31·5% *in vitro* recorded with conventional intracellular techniques (Dun & Mo, 1989). This might be due to several factors. Firstly, the better signal-to-noise ratio of the patch-clamp technique favours detection of small synaptic currents. Secondly, interneurones in the spinal cord are known to be quite sensitive to anoxic conditions (Davidoff, Shank, Graham, Aprison & Werman, 1967). The neurones of the neonatal animals used in our study may be more tolerant of anoxia than neurones from older animals. Finally, SPNs *in vivo* might be under tonic synaptic influence from higher brain regions. When cutting these synaptic inputs, one may release hitherto hidden synaptic events.

Number of channels involved in one synaptic event

Glycine receptor-gated Cl^- channels are reported to have conductance states between 17 and 79 pS (Bormann *et al.* 1987; Takahashi & Momiyama, 1991; Twyman & MacDonald, 1991). Taking these values the number of channels involved in the synaptic events can be roughly estimated. The smallest postsynaptic events that we observed at a V_h of -50 mV had amplitudes of about 15 pA. By assuming that the current is exclusively carried by glycine receptor-gated Cl^- channels in the lowest conductance state, we can calculate an upper limit of twenty channels involved in these events. The lower limit, calculated with the highest conductance state, is five channels for one of these events. Calculating for the 48 pS substate, which is reported to be the most frequent substate in rat dorsal horn IPSCs (Takahashi & Momiyama, 1991), gives a value of eight to nine channels for the smallest synaptic event. This is comparable to the values (ten to eighteen channels) Edwards, Konnerth & Sakmann (1990) found to underlie one quantal event of $GABA_A$-mediated IPSCs in granule cells of the dentate gyrus of rat hippocampus. Furthermore, if one assumes that the smallest synaptic current gives an estimate for the lowest quantal size in our preparation and neglecting an eventual non-linear summation of these events, this would imply that about 140 quanta are necessary to produce the largest synaptic currents we observed, involving the activation of 700–2800 channels.

Site of origin of synaptic currents

Since the dendritic processes of SPNs extend several hundred micrometres away from the cell soma (Bacon & Smith, 1988; Forehand, 1990), errors may arise from inadequate voltage control in these distal regions. If the synaptic currents we recorded originated in these regions, the time course and amplitude of these currents would probably be distorted by the filtering of the *RC* network of the distal dendrites.

The results of two recent studies (Chiba & Semba, 1991; Cabot *et al.* 1992) suggest that in the IML glycine receptors are more densely located on the membrane of the cell soma or the proximal, large dendrites rather than on distal, smaller dendrites. As a fairly good voltage control of these regions should be achieved under whole-cell recording conditions, the described size and decay time constants of the synaptic currents should also reflect, at least approximately, the real values. This is further supported by the fast rise time of the synaptic currents found in our study. However, we cannot definitely rule out a possible small distortion of size and decay time constant of the described synaptic currents.

Absence of spontaneous GABAergic synaptic currents

We found no indication of a spontaneous GABAergic synaptic regulation of SPN activity in our preparation. This was not expected in view of the presence of $GABA_A$ receptor-gated chloride channels on the membranes of these neurones, as demonstrated by other authors (Yoshimura & Nishi, 1982; Backman & Henry, 1983; Clendening & Hume, 1990) and in this study. A possible explanation would be to postulate the presence of GABAergic interneurones in our preparation which form synaptic contacts with SPNs but are not spontaneously active. Indeed, GABAergic interneurones have been shown to exist in the spinal cord (Magoul, Onteniente, Geffard & Calas, 1987; Todd & Sullivan, 1990). They are mostly located in laminae I–III of the dorsal horn. Yet, as there is little information about the location of interneurones projecting onto SPNs, it is not clear whether these GABAergic interneurones form synaptic contacts with SPNs. In fact, recent data (Cabot, Carroll & Alessi, 1991) provide some evidence against such a synaptic contact between GABAergic interneurones and SPNs. These authors injected wheat-germ agglutinin (WGA) into the superior cervical ganglion of rats. WGA retrogradely labelled SPNs in the IML, the central autonomic nucleus and the nucleus intercalatus. After WGA had crossed the synaptic cleft, they found in addition labelled interneurones in laminae IV, V and VII, but not in laminae I–III. In fact, our finding that 4-AP did not give rise to synaptic currents sensitive to SR95531 questions the existence of GABAergic interneurones projecting onto SPNs in a transverse slice preparation. Therefore, the hypothesis that $GABA_A$-receptor-gated Cl^- channels are activated by inputs not arising in the transverse slice might be more favourable. Indeed, morphological data (Bogan *et al.* 1986; Bacon & Smith, 1988) support the hypothesis of a supraspinal, GABAergic synaptic regulation of SPN activity. The cutting of these inputs during the preparation of transverse slices would explain the absence of spontaneous GABAergic synaptic activity in SPNs in a transverse spinal cord slice preparation, as was found by us and other authors (Dun & Mo, 1989).

I–V relationship of glycinergic IPSCs and neurotransmitter-induced currents

I–V relationships for exogenous application of glycine and GABA were linear over a wide range of membrane potentials, but displayed a weak outward rectification at highly depolarized membrane potentials when recorded under nominally equimolar Cl^- conditions. Outward rectification of GABA- and glycine-induced whole-cell currents has indeed been reported for mouse spinal cord neurones in Hepes-buffered extracellular solution (Bormann *et al.* 1987). However, we found a clear linear *I–V* relationship for glycinergic IPSCs in SPNs over the whole voltage range tested. In fact, such a linear *I–V* relationship has also been reported for glycine receptor-gated Cl^- channels in rat dorsal horn IPSCs (Takahashi & Momiyama, 1991) as well as for IPSCs in rat motoneurones (Takahashi, 1992). Like the present study, both studies have been performed in $NaHCO_3$-containing extracellular solutions. Also, a linear *I–V* relationship to exogenous application of glycine and GABA was reported for chicken embryonic SPNs (Clendening & Hume, 1990).

The difference in the *I–V* relationships for steady-state application of glycine and for glycinergic IPSCs may indicate that glycine receptor-gated Cl^- channels on the

postsynaptic site of a synaptic bouton are subjected to different environmental conditions from glycine receptor-gated Cl^- channels outside the synapse. In this respect, it has to be noted that we applied glycine and GABA exogenously in a Hepes-modified buffer without $NaHCO_3$. As glycine as well as GABA receptor-gated Cl^- channels are permeable to HCO_3^- and several other anions (Bormann *et al.* 1987), the different *I–V* relationships for exogenously applied agonist-induced and postsynaptic current may find an explanation herein. This also raises the interest in evaluating the relative permeability of HCO_3^- *versus* Cl^- in isolated patches from the SPNs.

Neurotransmitter effects

The present study shows that SPNs in a native, non-enzymatically treated rat spinal cord slice possess glycine and $GABA_A$ receptors that have physiological and pharmacological properties that are in general consistent with those found by other groups for these receptors (Clendening & Hume, 1990; Schneggenburger *et al.* 1992).

Run-down of neurotransmitter responses

The need for intracellular components to maintain or to modulate the function of the $GABA_A$ receptor (Chen, Stelzer, Kay & Wong, 1990) as well as the glycine receptor (Song & Huang, 1990) has previously been shown for cultured neurones. The run-down of the GABA responses seems in general to be slower and more heterogenous in duration in our preparation compared to the data for cultured neurones (Chen *et al.* 1990). This can partly be explained by the more extensive dendritic tree of a neurone in native tissue. In addition, other factors such as the presence of surrounding glia, supporting the intracellular homeostasis of the neurone, may be responsible. Although the more stable response to glycine when recording with ATP-containing intracellular solution suggests that there is also a need for intracellular components to maintain the glycine receptor in an entirely functional state, we have not found a run-down of glycine responses in all neurones recorded without ATP in the intracellular solution.

Physiological implications

Morphological (Bogan *et al.* 1986; Bacon & Smith, 1988; Cabot *et al.* 1992) as well as electrophysiological data (Yoshimura & Nishi, 1982; Backman & Henry, 1983; Clendening & Hume, 1990) show that at least two different inhibitory neurotransmitters can modulate SPN activity. Our data support these findings. Furthermore, the results we obtained in a non-enzymatically treated, transverse spinal cord slice suggest that *in vivo* glycine might be more strongly implicated in the intraspinal regulation of sympathetic body function, whereas GABA may be more likely to be used by higher brain regions and/or other spinal segments to modulate SPN activity.

Besides this differential control of SPN activity according to the neurotransmitters involved, the time course of the intraspinal synaptic activity may also be relevant for the regulation of the sympathetic system. In this respect, our observation of three different patterns of spontaneous synaptic activity is of interest.

Using conventional intracellular recordings in a neonatal spinal cord slice

preparation, Dun & Mo (1989) found IPSPs occurring at regular intervals in some of the recorded SPNs. In the same preparation, but using the patch-clamp technique, we found a comparable pattern of glycinergic IPSCs. Dun & Mo (1989) explain their finding by suggesting a rhythmicity of interneurones projecting onto the recorded SPNs. They suggest that in their preparation this rhythmicity has been revealed by the removal of descending inputs onto these interneurones. In fact, this explanation of an 'artificially' revealed rhythmicity has to be considered. Nevertheless, a rhythmic spiking activity has also been shown to be an intrinsic feature of some SPNs (Spanswick & Logan, 1990; Pickering *et al.* 1991). Interestingly, the frequencies described for the rhythmic spiking activity of SPNs are in the same range as the regular, glycinergic IPSCs observed in SPNs in our preparation. If we assume the existence of a functional Renshaw cell type of inhibition, as previously suggested for SPNs (Lebedev, Petrov & Skobelev, 1980; Dun & Mo, 1989), the same frequencies of SPN spiking activity and of glycinergic IPSCs might be explained by a rhythmically active SPN sending axon collaterals to a glycinergic interneurone. This interneurone then projects onto a second SPN, from which IPSCs occurring at regular intervals can be recorded. This would also explain the rare observation of this regularity in a transverse slice preparation, as its appearance would need a complete, functional Renshaw cell type circuitry.

Further studies will be needed to understand the complex integratory function of SPNs, as it is represented by the possible existence of a functional Renshaw cell type of inhibition in these neurones. Also, future experiments should help to test our hypothesis that glycine might be the more local, intraspinal inhibitory transmitter that modulates SPN activity, whereas GABA may be more likely to be used by higher brain regions and/or other spinal cord segments. In addition, GABA may regulate SPN activity not only by means of fast synaptic inputs, but also slowly at $GABA_B$ receptors or by metabolic changes of Cl^- gradients.

We wish to thank E. Desaulles, M. Poulter, B. Ribalet and R. Schlichter for helpful discussion and critical reading of the manuscript. M. E. Stoeckel gave helpful advice during morphological examination of the neurones. P. Vincent kindly supplied his program for detection of spontaneous synaptic currents. This research was supported by INSERM (CRE 9006–11) and Direction des Recherches, Etudes et Techniques (No. 91/131). J.K. is in receipt of a predoctoral fellowship of Boehringer Ingelheim Fonds.

REFERENCES

Backman, S. B. & Henry, J. L. (1983). Effects of GABA and glycine on sympathetic preganglionic neurons in the upper thoracic intermediolateral nucleus of the cat. *Brain Research* **277**, 365–369.

Bacon, S. J. & Smith, A. D. (1988). Preganglionic sympathetic neurones innervating the rat adrenal medulla: immunocytochemical evidence of synaptic input from nerve terminals containing substance P, GABA or 5-hydroxytryptamine. *Journal of the Autonomic Nervous System* **24**, 97–122.

Bacon, S. J., Zagon, A. & Smith, A. D. (1990). Electron microscopic evidence of a monosynaptic pathway between cells in the caudal raphé nuclei and sympathetic preganglionic neurons in the rat spinal cord. *Experimental Brain Research* **79**, 589–602.

Bogan, N., Mennone, A. & Cabot, J. (1986). Evidence for GABA-like immunoreactive input onto and surrounding retrogradely labelled sympathetic preganglionic neurones in the rat and pigeon. *Society for Neuroscience Abstracts* **12**, 1157.

BORMANN, J., HAMILL, O. P. & SAKMANN, B. (1987). Mechanism of anion permeation through channels gated by glycine and gamma-aminobutyric acid in mouse cultured neurones. *Journal of Physiology* **385**, 243–286.

CABOT, J. B. & BOGAN, N. (1987). Light microscopic observations on the morphology of sympathetic preganglionic neurons in the pigeon, *Columba livia*. *Neuroscience* **20**, 467–486.

CABOT, J. B., ALESSI, V. & BUSHNELL, A. (1992). Glycine-like immunoreactive input to sympathetic preganglionic neurons. *Brain Research* **571**, 1–18.

CABOT, J. B., CARROLL, J. & ALESSI, V. (1991). Localization of spinal cord interneurons with putative monosynaptic connections to sympathetic preganglionic neurons: a transneuronal transport study using wheat germ agglutinin. *Society for Neuroscience Abstracts* **17**, 339.

CHEN, Q. X., STELZER, A., KAY, A. R. & WONG, R. K. S. (1990). $GABA_A$ receptor function is regulated by phosphorylation in acutely dissociated guinea-pig hippocampal neurones. *Journal of Physiology* **420**, 207–221.

CHIBA, T. & SEMBA, R. (1991). Immuno-electronmicroscopic studies on the gamma-aminobutyric acid and glycine receptor in the intermediolateral nucleus of the thoracic spinal cord of rats and guinea pigs. *Journal of the Autonomic Nervous System* **36**, 173–182.

CLENDENING, B. & HUME, R. J. (1990). Expression of multiple neurotransmitter receptors by sympathetic preganglionic neurons in vitro. *Journal of Neuroscience* **10**, 3977–3991.

DAVIDOFF, R. A., SHANK, R. P., GRAHAM, L. T., APRISON, M. H. & WERMAN, R. (1967). Is glycine a neurotransmitter? *Nature* **214**, 680–681.

DEMBOWSKY, K., CZACHURSKI, J. & SELLER, H. (1985). An intracellular study of the synaptic input to sympathetic preganglionic neurones of the third thoracic segment of the cat. *Journal of the Autonomic Nervous System* **13**, 201–244.

DUN, N. J. & MO, N. (1989). Inhibitory postsynaptic potentials in neonatal rat sympathetic preganglionic neurones *in vitro*. *Journal of Physiology* **410**, 267–281.

EDWARDS, F. A., KONNERTH, A. & SAKMANN, B. (1990). Quantal analysis of inhibitory synaptic transmission in the dentate gyrus of rat hippocampal slices: a patch-clamp study. *Journal of Physiology* **430**, 213–249.

EDWARDS, F. A., KONNERTH, A., SAKMANN, B. & TAKAHASHI, T. (1989). A thin slice preparation for patch clamp recordings from neurones of the mammalian central nervous system. *Pflügers Archiv* **414**, 600–612.

FOREHAND, C. J. (1990). Morphology of sympathetic preganglionic neurons in the neonatal rat spinal cord: an intracellular horseradish peroxidase study. *Journal of Comparative Neurology* **298**, 334–342.

GRACE, A. A. & LLINÁS, R. (1985). Morphological artifacts induced in intracellularly stained neurons by dehydration: circumvention using rapid dimethyl sulfoxide clearing. *Neuroscience* **16**, 461–475.

HAMANN, M., DESARMENIEN, M., DESAULLES, E., BADER, M. F. & FELTZ, P. (1988). Quantitative evaluation of the properties of a pyridazinyl $GABA_A$ derivative (SR95531) as a $GABA_A$ competitive antagonist. An electrophysiological approach. *Brain Research* **442**, 287–296.

HAMILL, O. P., MARTY, A., NEHER, E., SAKMANN, B. & SIGWORTH, F. J. (1981). Improved patch-clamp techniques for high-resolution current recording from cells and cell-free membrane patches. *Pflügers Archiv* **391**, 85–100.

HENRY, J. L. & CALARESU, F. R. (1974). Pathways from medullary nuclei to spinal cardio-acceleratory neurones in the cat. *Experimental Brain Research* **20**, 505–514.

LASKEY, W. & POLOSA, C. (1988). Characteristics of the sympathetic preganglionic neuron and its synaptic input. *Progress in Neurobiology* **31**, 47–84.

LEBEDEV, V. P., PETROV, V. J. & SKOBELEV, V. A. (1980). Do sympathetic preganglionic neurones have a recurrent inhibitory mechanism? *Pflügers Archiv* **383**, 91–97.

LOEWY, A. D., MCKELLAR, S. & SAPER, C. B. (1979). Direct projections from the A5 catecholamine cell group to the intermediolateral cell column. *Brain Research* **174**, 309–314.

MCCALL, R. B. (1988). Effects of putative neurotransmitters on sympathetic preganglionic neurons. *Annual Review of Physiology* **50**, 553–564.

MAGOUL, R., ONTENIENTE, B., GEFFARD, M. & CALAS, A. (1987). Anatomical distribution and ultrastructural organisation of the GABAergic system in the rat spinal cord: an immuno-histochemical study using anti-GABA antibodies. *Neuroscience* **20**, 1001–1009.

Mo, N. & Dun, N. J. (1987). Is glycine an inhibitory transmitter in rat lateral horn cells? *Brain Research* **400**, 139–144.

Olsen, R. W. (1982). Drug interactions at the GABA receptor–iontophore complex. *Annual Review of Pharmacology and Toxicology* **22**, 245–277.

Pickering, A. E., Spanswick, D. & Logan, S. D. (1991). Whole-cell recording from sympathetic preganglionic neurons in rat spinal cord slices. *Neuroscience Letters* **130**, 237–242.

Saper, C. B., Loewy, A. D., Swanson, L. W. & Cowan, W. M. (1976). Direct hypothalamo-autonomic connections. *Brain Research* **117**, 305–312.

Schneggenburger, R., López-Barneo, J. & Konnerth, A. (1992). Excitatory and inhibitory synaptic currents and receptors in rat medial septal neurones. *Journal of Physiology* **445**, 261–276.

Shen, E. & Dun, N. J. (1990). Neonate rat sympathetic preganglionic neurons intracellularly labelled with lucifer yellow in thin spinal cord slices. *Journal of the Autonomic Nervous System* **29**, 247–254.

Song, Y. & Huang, L.-Y. M. (1990). Modulation of glycine receptor chloride channels by cAMP-dependent protein kinase in spinal trigeminal neurons. *Nature* **348**, 242–245.

Spanswick, D. & Logan, S. D. (1990). Spontaneous rhythmic activity in the intermediolateral cell nucleus of the neonate rat thoraco-lumbar spinal cord *in vitro*. *Neuroscience* **39**, 395–403.

Swanson, L. W. (1977). Immunohistochemical evidence for a neurophysin-containing autonomic pathway arising in the paraventricular nucleus of the hypothalamus. *Brain Research* **128**, 346–353.

Takahashi, T. (1978). Intracellular recording from visually identified motoneurones in rat spinal cord slices. *Proceedings of the Royal Society* B **202**, 417–421.

Takahashi, T. (1990). Membrane currents in visually identified motoneurones of neonatal rat spinal cord. *Journal of Physiology* **423**, 27–46.

Takahashi, T. (1992). The minimal inhibitory synaptic currents evoked in neonatal rat motoneurones. *Journal of Physiology* **450**, 593–611.

Takahashi, T. & Momiyama, A. (1991). Single-channel currents underlying glycinergic inhibitory postsynaptic responses in spinal neurones. *Neuron* **7**, 965–969.

Todd, A. J. & Sullivan, A. C. (1990). Light microscopic study of the coexistence of GABA-like and glycine-like immunoreactivities in the spinal cord of the rat. *Journal of Comparative Neurology* **296**, 496–505.

Twyman, R. E. & MacDonald, R. L. (1991). Kinetic properties of the glycine receptor main- and sub-conductance states of mouse spinal cord neurones in culture. *Journal of Physiology* **435**, 303–331.

Yoshimura, M. & Nishi, S. (1982). Intracellular recordings from lateral horn cells of the spinal cord in vitro. *Journal of the Autonomic Nervous System* **6**, 5–11.